

1 **The effects of pre-ignition turbulence by gas jets on the explosion behavior**
2 **of methane-oxygen mixtures**

3
4 Xinyu Chang¹, Bo Zhang^{2†}, Hoi Dick Ng³, Chunhua Bai¹

5 ¹Beijing Institute of Technology
6 State Key Laboratory of Explosion Science and Technology, Beijing 100081, China

7 ²Shanghai Jiao Tong University
8 School of Aeronautics and Astronautics, Shanghai, 200240, China

9 ³Concordia University
10 Department of Mechanical, Industrial and Aerospace Engineering
11 Montréal, QC, H3G 1M8, Canada

12
13 [†]Corresponding Author
14 Shanghai Jiao Tong University
15 School of Aeronautics and Astronautics, Shanghai, 200240, China
16 E-mail: bozhang@sjtu.edu.cn

17
18
19
20
21
22
23
24
25
26
27
28
29
30
31
32
33
34
35
36
37
38

The effects of pre-ignition turbulence by gas jets on the explosion behavior of methane-oxygen mixtures

Abstract

Most of the previous studies investigating explosion characteristics of combustible mixtures were performed at quiescent state. However, in realistic accidental explosion scenarios, the ignition of the combustible mixture usually occurs under a turbulent environment. In this study, we examine the maximum explosion pressure p_{\max} and explosion time τ_e of CH₄-2O₂ mixtures under the pre-ignition turbulence condition in a spherical closed chamber at a room temperature of 298 K. Turbulence is generated using fluidic jet of three different gases (O₂, CO₂ and N₂) and its intensity is controlled by changing the initial pressure of the gas jet p_{J0} (i.e., 200 and 500 kPa) and the explosion chamber pressure p_0 (i.e., 40 and 60 kPa). The dual effects of turbulence and gas dilution on the explosion behavior of CH₄-2O₂ mixtures are investigated in detail. The results indicate that by adding O₂ into CH₄-2O₂ mixture at quiescent condition, p_{\max} increases but the rate of overpressure rise is reduced. By introducing turbulence through gas jets into the combustible mixture, the explosion behavior is affected by both the turbulence and gas dilution. With O₂ injection, turbulence overall enhances the explosion, but the amount of O₂ dilution increases at higher p_{J0}/p_0 and longer jet duration time (t_{J0}), rendering the mixture to tend toward fuel-lean side and slow down the explosion rate. The present results also demonstrate that the turbulence effect of CO₂ is more profound than that of N₂ jet. Both p_{\max} and τ_e are enhanced by CO₂ jet turbulence when t_{J0} is relative short ($t_{J0} < 400$ ms). However, for longer t_{J0} , the dominance of CO₂ dilution becomes more noticeably than N₂ dilution with a longer explosion time τ_e .

Keywords: Turbulence; Fluidic jet; Gas dilution; Explosion; Methane

63 1. Introduction

64 Methane (CH₄) is a hydrocarbon fuel widely used in multitudinous fields. Its use in power
65 generation has long been considered as a “cleaner” alternative to other fossil fuels or coal [1]. Not
66 only is the main component of natural gas, methane can also be produced from biomass providing a
67 renewable source of energy. As a combustible fuel source, the flammability and explosion hazards
68 of methane are of great concern concerning its transportation and storage. As such, numerous inves-
69 tigation have been performed on the combustion and explosion characteristics of methane-based
70 mixtures, e.g., [2-14]. Recently, the detonation propagation and its limits [15-24] have been widely
71 investigated regarding methane mixtures due to their possible applications in detonation-based en-
72 gines.

73 In research, the 20-L explosion spherical vessel has become the standard apparatus to evaluate
74 explosion properties of gases/vapors [25], dusts [26], hybrid dust-gas/vapor mixtures [27]. Meas-
75 urement includes the flammability limits, limiting oxygen concentration, minimum ignition energy,
76 maximum explosion pressure p_{\max} , maximum rate of pressure rise $(dp/dt)_{\max}$, explosion time τ_e and
77 laminar burning velocity S_L [28-36].

78 To either enhance the combustion efficiency or mitigate explosion hazards, different fuels or
79 inert gases can be blended into methane-based mixtures. For instance, Wang *et al.* [37] suggested
80 that hydrogen addition can improve the flame speed and decrease the combustion duration notably,
81 while p_{\max} is not significantly affected. Ma *et al.* [38] and Wierzba *et al.* [39] showed that the ex-
82 plosion intensity can be enhanced by hydrogen addition; parameters such as p_{\max} , $(dp/dt)_{\max}$ and
83 temperature increase with increasing hydrogen content in the methane-hydrogen-air mixture. Sarli
84 *et al.* [40, 41] discussed the scenario that hydrogen addition to methane can lead to a more vigorous
85 flame/turbulence interaction, which was the underlying factor being responsible for the explosion

86 process of hydrogen-methane/air mixtures. Mitu *et al.* [42] investigated the ignition temperatures of
87 flammable substances in ($N_2 + O_2$) mixtures with different concentrations of oxygen. On the other
88 hand, the explosion behavior can be suppressed by inert gas dilution. Zhang *et al.* [31] showed that
89 addition of argon Ar or nitrogen N_2 into dimethyl ether-air mixture can result in a decrease of p_{max} .
90 Compared with Ar dilution, the decrease of S_L is faster when the mixture is diluted with N_2 . Shen *et*
91 *al.* [43] examined explosion hazards of $C_2H_4-N_2O$ mixtures with N_2 or CO_2 addition. They found
92 that dilutions by N_2 and CO_2 restrict the decomposition of N_2O by enhancing tri-molecular reaction.
93 Zhou *et al.* [44] argued that N_2 and CO_2 dilutions also have an important impact on S_L and flame
94 instability in $H_2/CO/CH_4$ /air mixtures. Their studies showed that the thermal and chemical effects of
95 CO_2 dilution is greater than those of N_2 . Mitu *et al.* [45] investigated the effectiveness of diluent
96 gases on explosion characteristics. The experimental results showed that CO_2 was the most effective
97 gas, followed by H_2O , exhaust gas, and N_2 . Benedetto *et al.* [46] analyzed the effects induced by the
98 additionally introduced inert gases (CO_2 , N_2 , He, and Ar) on the explosion behavior of $CH_4/O_2/N_2$
99 mixtures, they found that the inhibition effects of those inert gases on the explosion parameters in
100 combustible mixtures were in the order of CO_2 , N_2 , He and Ar.

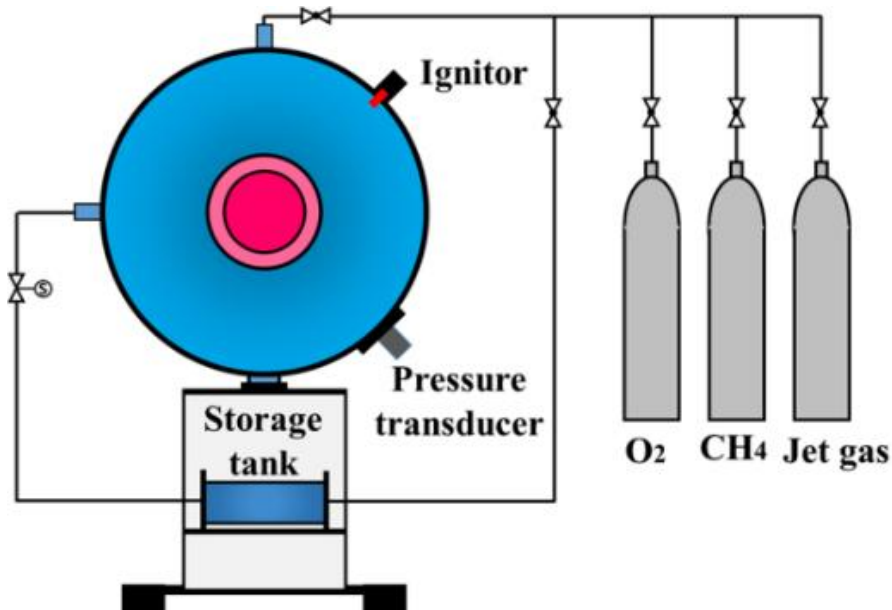
101 Despite a wealth of studies on the explosion behavior of methane-related mixtures, the majori-
102 ty has obtained results with mixtures initially at quiescent state. In real explosion scenarios, the
103 combustible is usually subject to a turbulent flow environment caused by wind or obstacles. In re-
104 cent years, research has focused on the important role of turbulence on the explosion process [47,
105 48]. Benedetto *et al.* [49] demonstrated the influence of turbulence on the explosion characteristics
106 of hybrid mixtures of methane and nicotinic acid, such as the maximum pressure, deflagration index,
107 and minimum ignition energy. Sun & Li [50] investigated the effects of initial turbulence on the ex-
108 plosion of hydrogen-air mixtures by comparing the explosion parameters under both laminar and

109 turbulent ambiances. Bauwens & Dorofeev [51] carefully examined the initial turbulence on vented
110 explosion overpressures. Kundu *et al.* [52] investigated the effect of turbulence and explosive pow-
111 ders in a confined explosion using a 1-m³ large-scale spherical apparatus.

112 In most experimental settings, turbulence is typically generated by injecting a gas into the
113 combustible. Hence, turbulence intensity and the nature of the turbulence-generating gas could both
114 affect the explosion process. Up-to-date, no extensive investigation has yet taken into account the
115 combined effect of turbulence and gas dilution. Hence, in this work, this combined effect of
116 pre-ignition turbulence generated by three different gases on the explosion characteristics, i.e., p_{\max} ,
117 and τ_e , are systematically determined.

118

119 2. Experimental setup



120

121 **Fig.1** A sketch of the experimental setup.

122

123 The experimental setup consisted of a standard 20-L explosion spherical vessel, high-voltage
124 ignition system, fluidic jet generation device, time-delay control and data acquisition system (Fig.
125 1). The vessel has a 33.68-cm inner diameter and 10-mm thickness. For turbulence generation, high

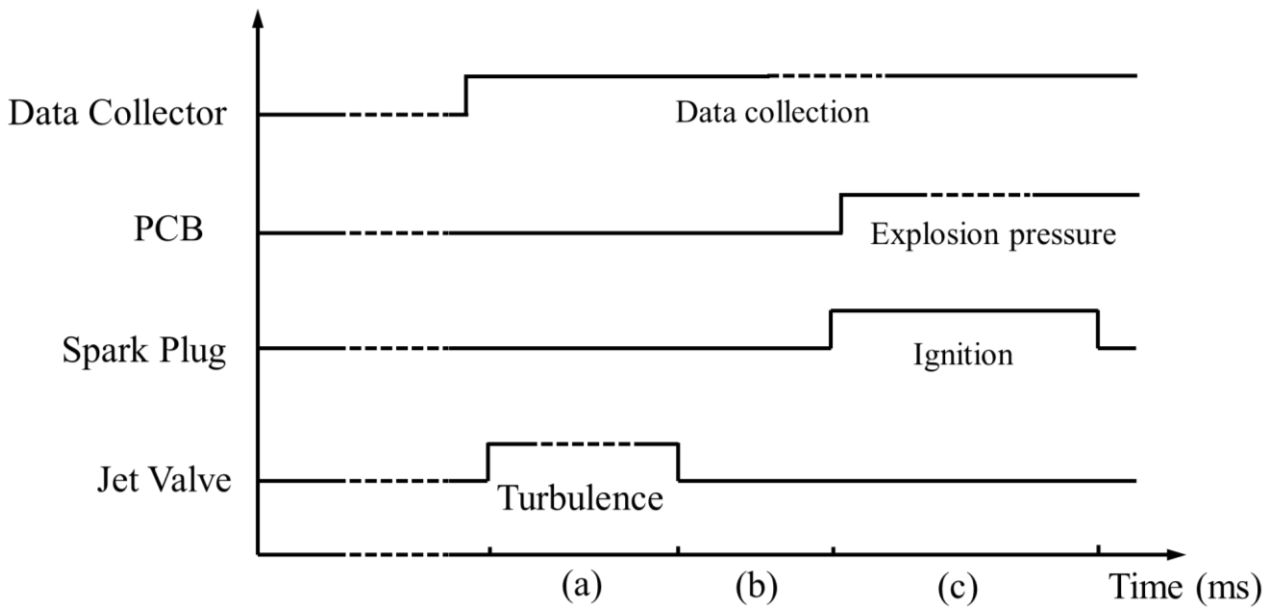
126 pressure gas from a 3.1-L tank was promptly injected into the chamber via a solenoid valve. Omega
127 pressure gauges (PXM309, 0-0.7 MPa range and accuracy $\pm 0.25\%$ of full scale) were used to mon-
128 itor the initial pressure. The $\text{CH}_4\text{-2O}_2$ mixture was ignited by an ignitor mounted at the upper part of
129 the spherical vessel, and two electrodes extended into the chamber with a depth of 1 cm.

130 For each experiment, the explosion vessel was first evacuated below 100 Pa. Afterwards, me-
131 thane and oxygen were filled into the vessel to the desired condition by the method of partial pres-
132 sures and left intact for at least 10 minutes to ensure a quiescent well-mixed mixture. The methane
133 volume fraction χ_{CH_4} is defined as $\chi_{\text{CH}_4} = V_{\text{CH}_4} / (V_{\text{O}_2} + V_{\text{CH}_4})$ where V_{CH_4} the methane volume and
134 V_{O_2} the oxygen volume. Another tank was filled with a specific gas (O_2 , CO_2 or N_2) to a high pres-
135 sure for injection (200 or 500 kPa). The delay control system arranged the time sequence of fluidic
136 jet generation and ignition. As shown in Fig. 2, when the system was triggered, it sent pulse signals
137 to activate the solenoid valve producing a gas jet from the high-pressure tank, and the jet duration
138 time t_{j0} can be adjusted accordingly, ranging from 20 to 800 ms. After a delay time t_d of 100 ms, the
139 combustible mixture under the turbulent condition was ignited by a spark plug with low energy in
140 order to avoid additional turbulence induced by ignition energy. In this study, t_d was defined as the
141 time period starting from the end of the jet flow to the beginning of the ignition. The pressure evo-
142 lution inside the explosion chamber was recorded by a PCB transducer (113B21), from which two
143 explosion parameters (p_{max} and τ_e) were determined. Here, τ_e was defined as the period from igni-
144 tion to the time when the explosion pressure reaches its peak. The initial temperature was 298 K for
145 all experiments. Figure 3 shows a sample explosion pressure data obtained from the experiment. To
146 extract p_{max} and τ_e , the raw trajectory was first processed by a smoothing technique using a Gaussi-
147 an-weighted moving average filter [21].

148 Experimental errors in this study can be summarized to two major categories: the random error

149 and the systematic error. In this study, the random error mainly originated from the measurement of
 150 the explosion trajectory, which is due to the transient nature of explosion process. At least three
 151 shots were repeated for each condition, and the explosion overpressure trajectories were reproduc-
 152 ble because the results fluctuated within 5 %. In order to guarantee the accuracy of the experimental
 153 results, the explosion parameters (i.e., p_{\max} , τ_e) presented in this work were calculated from the av-
 154 erage values of three shots. Systematic error mainly resulted from Omega pressure gauge (PXM309)
 155 used to measure the initial pressure, which ranged from 0 to 0.7 MPa with an accuracy of ± 0.25 %
 156 of full scale, and hence the maximum error of initial pressure measurement was to be approximately
 157 ± 1.75 kPa.

158



159

Fig. 2 An illustration of timing for system components.

160

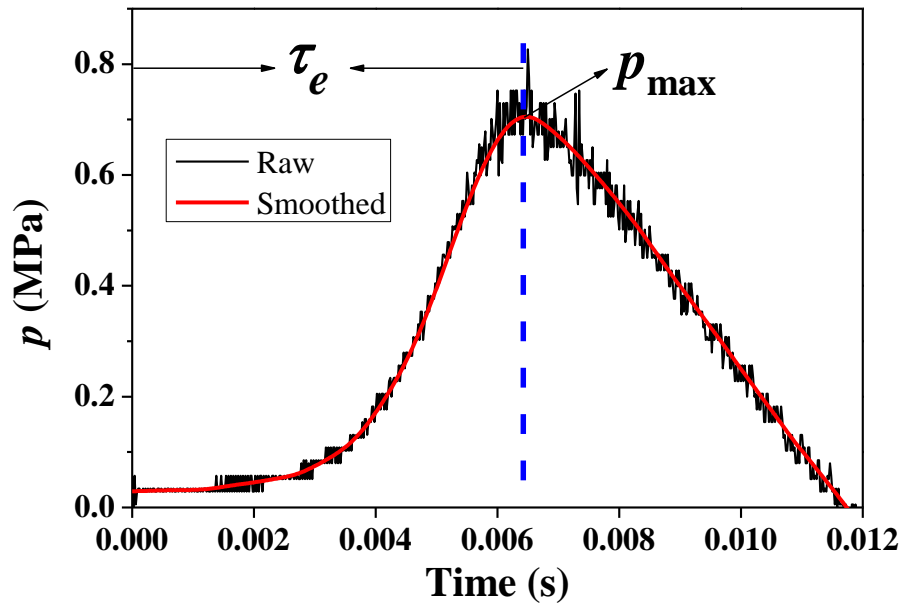
161

a) t_{j0} (ranging from 20~800 ms), b) t_d (100 ms), c) ignition time t_i (200 ms).

162

163

164



165

166 **Fig. 3** Comparison of the raw pressure data and curve after smoothing ($\phi = 1.0$, $p_0 = 60$ kPa, quiescent state).

167

168

169 3. Results and Discussion

170 3.1 Experiments without initial turbulence

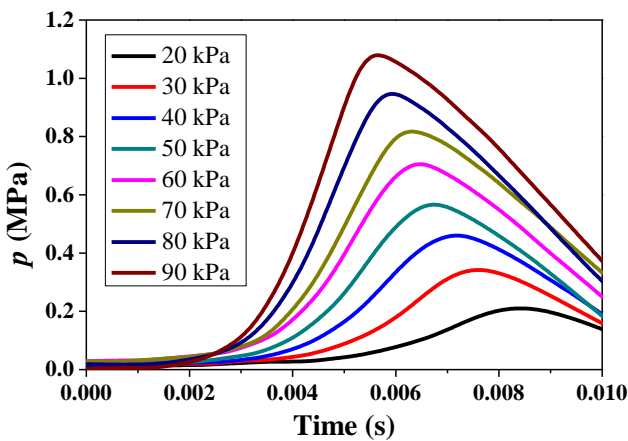
171 Figure 4a shows the explosion pressure trajectories of $\text{CH}_4\text{-O}_2$ under quiescent condition with

172 p_0 from 20 to 90 kPa. For $p_0 = 20$ kPa, p_{max} is 0.21 MPa and τ_e is 8.5 ms. When p_0 increases to 50

173 kPa, p_{max} increases but τ_e decreases. The corresponding values are 0.58 MPa and 6.7 ms, respec-

174 tively. As p_0 increases further to 90 kPa, p_{max} reaches 1.08 MPa with τ_e equal to 5.7 ms. Both the

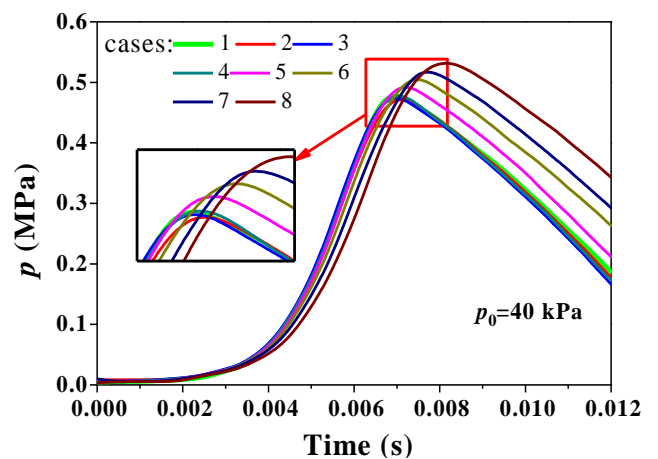
175 maximum pressure and the rate of pressure rise can be observed to increase with p_0 .



176

177

(a)



(b)

178 **Fig. 4** Explosion pressure evolution for CH₄-2O₂ mixture initially at quiescent state. a) with various p_0 and b)
 179 diluting with different O₂ amount at $p_0=40$ kPa.
 180

181 **Table 1** O₂ dilution for cases with $p_0=40$ kPa and $p_{J0}=500$ kPa

Case No.	1	2	3	4	5	6	7	8
t_{J0} (ms)	0	20	50	100	200	400	600	800
p_1 (kPa)	40	40.40	40.89	41.67	43.57	46.46	49.57	52.29
V_{O_2} (L)	0	0.08	0.18	0.33	0.71	1.28	1.90	2.43
χ_{CH_4} (%)	33.3	33.0	32.6	32.0	30.6	28.7	26.9	25.5
φ	1	0.99	0.97	0.94	0.88	0.81	0.74	0.68

182
 183 After the fluidic jet emerges into the chamber, the explosion characteristics of the tested mix-
 184 ture are affected by two factors: turbulence and the injected gas. For the latter, it is equivalent to
 185 adding a certain O₂ amount into the CH₄-2O₂ mixture. Hence, the effective mixture φ tends to the
 186 fuel-lean side if the added O₂ is considered. For jet duration t_{J0} ranging from 0 to 800 ms, the initial
 187 chamber pressure increases while both χ_{CH_4} and φ decrease, which can be determined by calculating
 188 the remaining O₂ volume in the storage tank. Table 1 summarizes the parameters after O₂ injection,
 189 including the initial chamber pressure p_0 and high-pressure tank for the jet generation p_{J0} , the
 190 chamber pressure after the O₂ injection p_1 , the volume of oxygen dilution V_{O_2} , the mole fraction of
 191 CH₄ after injection χ_{CH_4} , and the equivalent ratio φ .

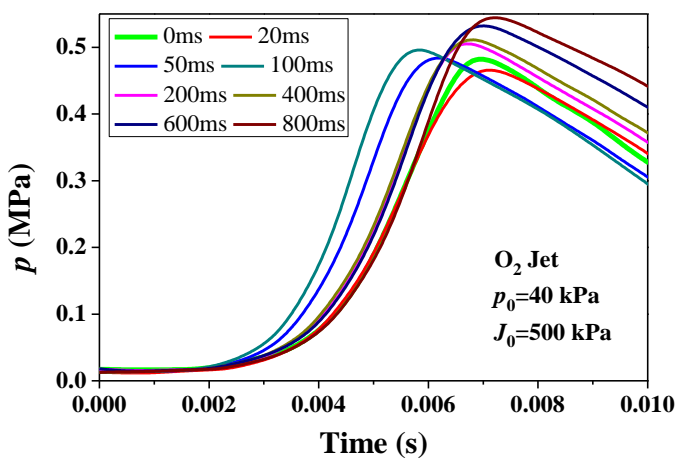
192 The explosion pressure data for different cases of O₂ addition are shown in Fig. 4b. For these
 193 shots, O₂ was added into the chamber and the mixture was ignited after 10 minutes. Therefore, the
 194 results are considered to be measured at quiescent state without any turbulence effect to investigate
 195 only the O₂ dilution on the explosion behavior of methane-oxygen mixtures.

196 In Fig. 4b, the values of p_{max} and τ_e hold on for cases 1 to 4 (for t_{J0} from 0 to 100 ms). It thus
 197 indicates that adding small amount of O₂ plays little impact on the explosion behavior. As t_{J0} in-
 198 creases from 200 to 800 ms (cases 5 to 8), p_{max} increases from 0.48 to 0.53 MPa, and τ_e increases
 199 from 7.0 to 8.1 ms, accordingly. Hence, a relatively large amount of O₂ dilution can increase both

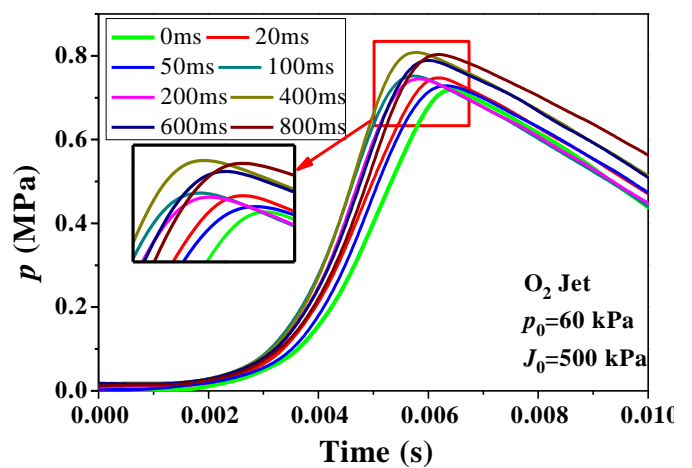
200 p_{\max} and τ_c . In other words, the added oxygen increases the overpressure, but it slows down the rate
 201 of pressure rise. It is noteworthy that, by adding the amount of O₂ into the mixture, the initial pres-
 202 sure insider the chamber is also increased, e.g., when the jet duration time (t_{j0}) increases from 0 to
 203 800 ms, the initial pressure increases from 40 kPa to 52.3 kPa (shown in Table 1), Fig.4a shows an
 204 increase in the initial pressure results in an increase of overpressure and pressure rise rate. Zhang et
 205 al. [53] suggested that an increase in the initial pressure could result in a decrease in the distance
 206 between molecules, increasing the incidence of collision of molecules, thereby accelerating the
 207 chemical reaction rate, and p_{\max} accordingly increases. The above analysis suggests that there is a
 208 combination effect induced by adding certain amount of O₂ into the mixture (viz. the dilution ac-
 209 companied by the decrease of equivalence ratio and the increase of total initial pressure), eventually
 210 resulting in increasing the overpressure but slowing down the rate of pressure rise.

211

212 **3.2 Effect of turbulence generated by O₂ jet**



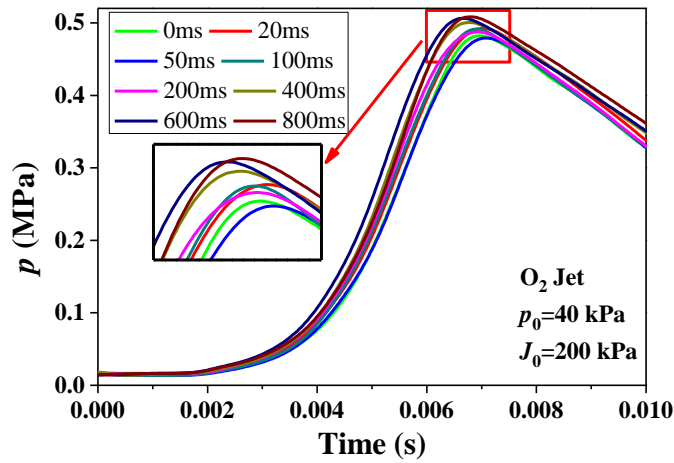
(a)



(b)

213

214



(c)

Fig. 5 Explosion pressure evolution with O₂ jet turbulence.

215

216

217

218

219

220

221

222

223

224

225

226

227

228

229

230

231

232

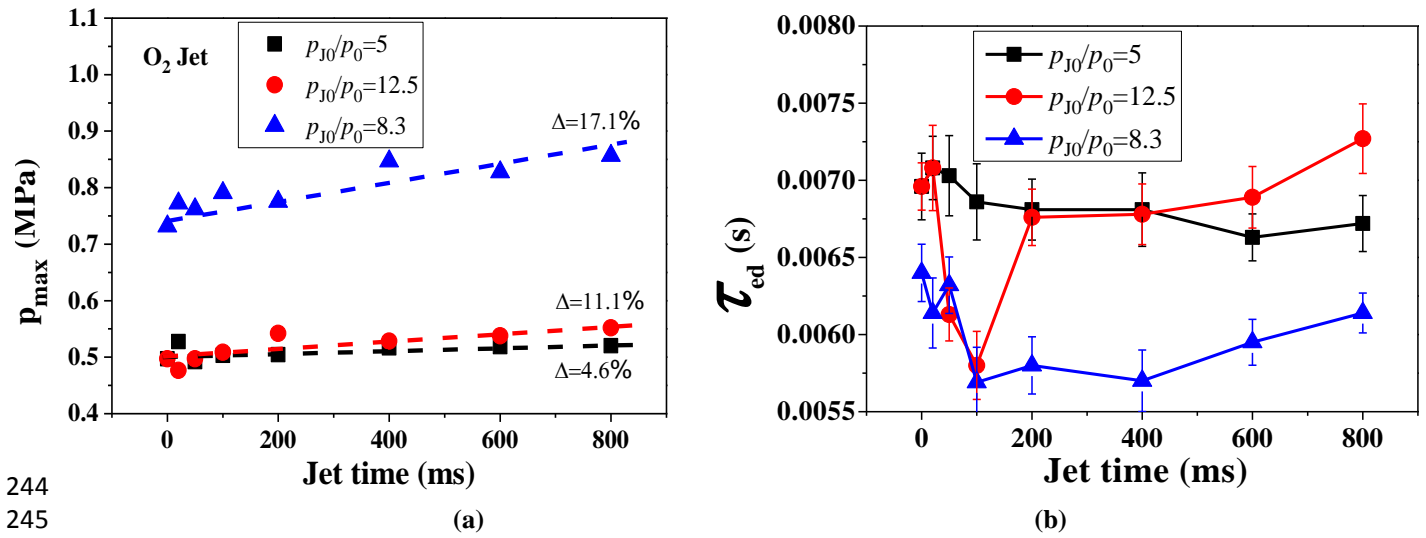
233

In this study, the pressure difference between high-pressure storage tank and the explosion chamber is the primary factor that influences the turbulence intensity, i.e., p_{J0}/p_0 , the higher p_{J0}/p_0 is, the higher the turbulence intensity will be. Figure 5 shows the pressure trajectories with turbulence effect generated by an O₂ jet. For Fig. 5a, $p_0 = 40$ kPa and $p_{J0} = 500$ kPa (hence, $p_{J0}/p_0 = 12.5$), while t_{J0} varies from 0 to 800 ms. When t_{J0} increases from 0 to 100 ms, p_{max} varies slightly from 0.47 to 0.50 MPa, while the value of τ_e is greatly reduced (i.e., from 7.0 to 5.9 ms). As illustrated in Fig. 4b, adding the same amount of O₂ but without the turbulence has little impact on p_{max} and τ_e . While with turbulence (Fig. 5a), although p_{max} does not change significantly, τ_e is greatly reduced by 15.7 %. When t_{J0} increases from 200 to 800 ms, p_{max} consistently increases (from 0.51 to 0.54 MPa). However, in contrast to the small volume injection (t_{J0} equal to 0 to 100 ms), τ_e also increases from 6.7 to 7.2 ms, indicating the explosion pressure rise rate is lowered. This behavior is similar as that without turbulence (Fig. 4b). From Table 1 and Fig. 4b, as t_{J0} increases from 200 to 800 ms, the volume of O₂ added into the chamber increases from 0.71 to 2.43 L and ϕ changes from 0.88 to 0.68. Although the explosion characteristics are promoted by the turbulence, the influence of high O₂ dilution is more significant, which reduces the explosion reaction rate, thus increasing τ_e .

234 Figure 5b shows results for $p_0 = 60$ kPa and $p_{J0} = 500$ kPa ($p_{J0}/p_0 = 8.3$). In this case, the turbu-
 235 lence intensity is reduced. It is observed that, when t_{J0} goes up to 800 ms, the value of p_{\max} also in-
 236 creases from 0.72 to 0.81 MPa, and τ_e persistently decreases from 7.0 to 6.2 ms. This suggests that
 237 both the effects of turbulence and O₂ dilution promote the explosion characteristics with increasing
 238 p_{\max} and decreasing τ_e .

239 Results for $p_0 = 40$ kPa and $p_{J0} = 200$ kPa ($p_{J0}/p_0 = 5$) are shown in Fig. 5c. Note that the tur-
 240 bulence intensity for this case is relatively weak compared to the previous two cases. There is no
 241 obvious variation for both p_{\max} and τ_e , indicating a competing effect between turbulence and O₂ di-
 242 lution and hence, results in little impact on the explosion behavior.

243



244

245

246 **Fig. 6** Explosion parameters a) p_{\max} and b) τ_e as a function of t_{J0} with O₂ jet turbulence.

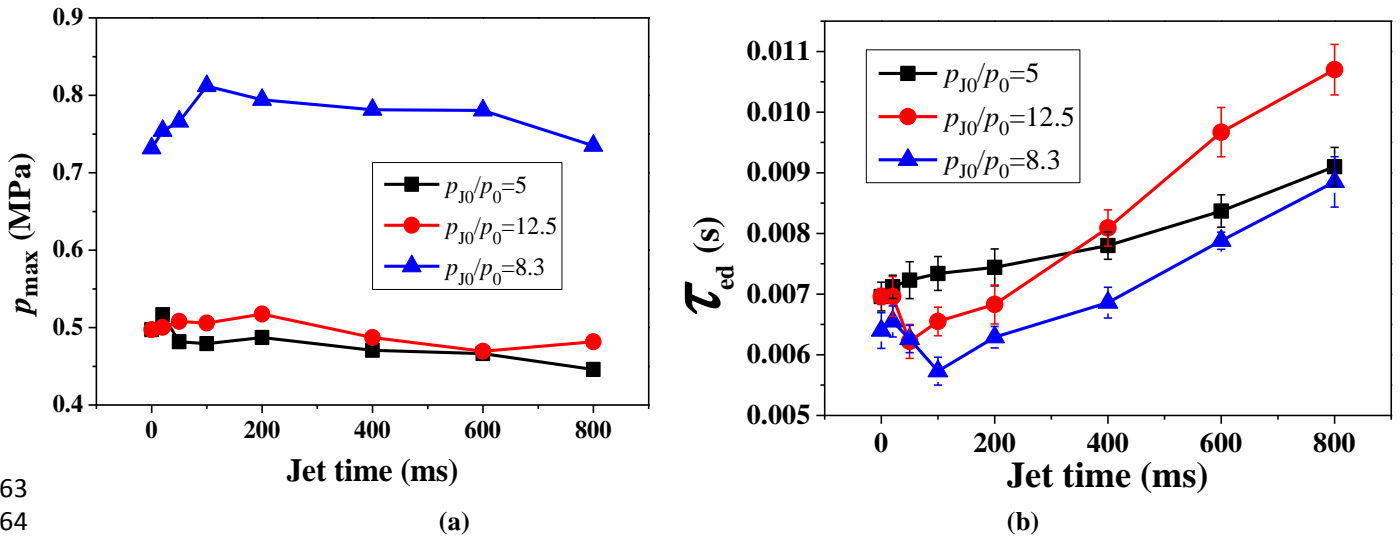
247

248 Figure 6 summaries p_{\max} and τ_e results with varying t_{J0} for $p_{J0}/p_0 = 12.5, 8.3$ and 5. For each in-
 249 dividual case, there exists a linear increase between p_{\max} and t_{J0} . As t_{J0} goes from 0 to 800 ms, p_{\max}
 250 increases by 11.1% for $p_{J0}/p_0 = 12.5$, and 17.1% and 4.6% for $p_{J0}/p_0 = 8.3$ and 5, respectively. At
 251 high turbulence conditions ($p_{J0}/p_0 = 12.5$ and 8.3) and short injection time t_{J0} , the explosion time τ_e
 252 is reduced (especial for $p_{J0}/p_0 = 12.5$). Hence, the combustion rate is promoted at those conditions.

253 However, for higher t_{j0} , the resulting increase of O_2 dilution into the mixture becomes prominent
 254 and this effect suppresses the explosion rate, hence resulting in an increasing τ_e . These results illus-
 255 trate that there is an opposite effect between turbulence and O_2 dilution, both affecting the explosion
 256 behavior in a confined chamber. For higher the p_{j0}/p_0 , the stronger the turbulence intensity is, which
 257 promotes the chemical reaction, burning velocities and the explosion overpressure via distorting and
 258 expanding the flame surface area [54]. In contrast, with increasing jet duration time, hence, O_2 addi-
 259 tion amount, the mixture tends to the fuel-lean side which suppresses the explosion rate to some ex-
 260 tent.

261

262 3.3 Effect of turbulence generated by inert gases



263

264

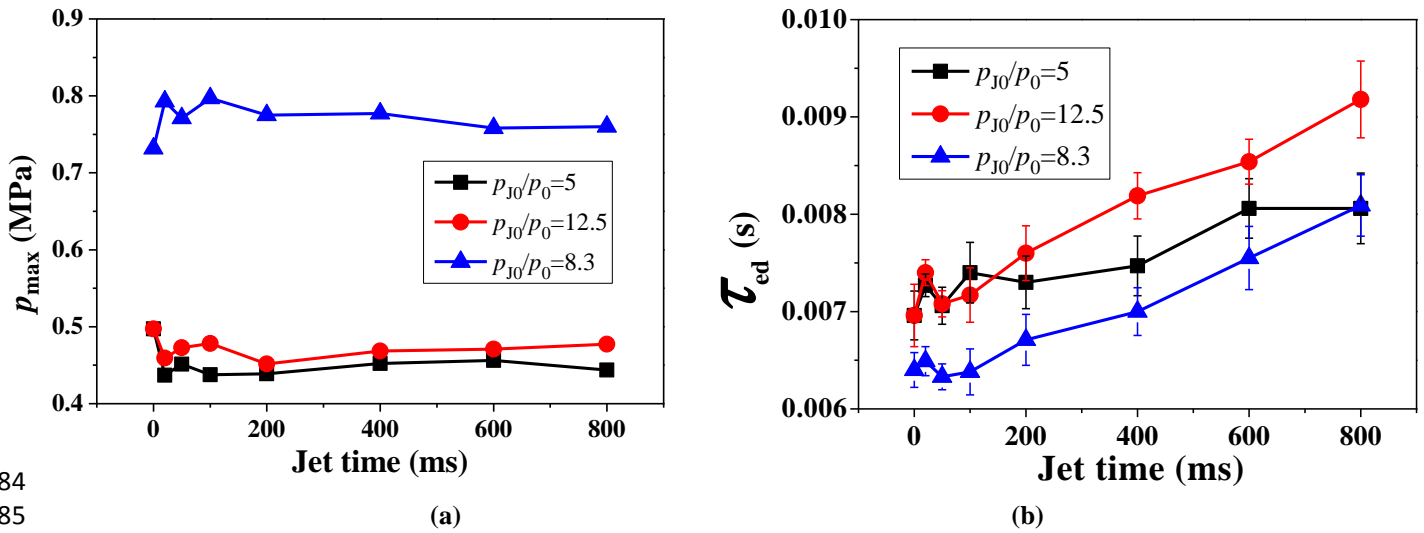
265 **Fig. 7** Explosion parameters a) p_{max} and b) τ_e as a function of t_{j0} with CO_2 jet turbulence.

266

267 For the O_2 injection, besides the generated turbulence affecting the explosion behavior, the in-
 268 creased χ_{O_2} also influences the chemical reaction rate and the explosion process. Here we further
 269 investigate the turbulence effect by inert gases on the CH_4 - $2O_2$ explosion behavior. Previous inves-
 270 tigation [32, 55-57] illustrated that unreactive gases have significant suppression effects on the ex-
 271 plosion process. Figure 7 shows that for $p_{j0}/p_0 = 5$, with increasing t_{j0} from 0 to 800 ms the expo-

272 sion hazard is relaxed, i.e., p_{\max} decreases and τ_e increases. For $p_{J0}/p_0 = 12.5$, p_{\max} generally keeps
 273 constant and τ_e first decreases and afterwards it quickly goes up, indicating the explosion hazard is
 274 in turn inhibited. Lastly, for the case of $p_{J0}/p_0 = 8.3$, p_{\max} first increases to 0.81 MPa and then decays
 275 to the state equivalent to that without turbulence ($p_{\max} = 0.73$ MPa). Similar to the $p_{J0}/p_0 = 12.5$ case,
 276 τ_e decays and then increases. For this last case, the turbulence first promotes the explosion but the
 277 CO_2 dilution quickly balances this positive effect as t_{J0} is increasing to 800 ms. The reason that the
 278 results from $p_{J0}/p_0 = 8.3$ are different from the cases of $p_{J0}/p_0 = 5$ and 12.5 is mainly because the ini-
 279 tial pressure for test is different, i.e., for the cases of $p_{J0}/p_0 = 5$ and 12.5, the p_0 is 40 kPa, while for
 280 $p_{J0}/p_0 = 8.3$, the corresponding p_0 is 60 kPa. Results have clarified that the increase in the initial
 281 pressure could accelerate the chemical reaction rate and increase in explosion pressure. Therefore,
 282 the baseline of p_{\max} is much higher for $p_{J0}/p_0 = 8.3$ than other cases.

283



284

285

286 **Fig. 8** Explosion parameters a) p_{\max} and b) τ_e as a function of t_{J0} with N_2 jet turbulence.

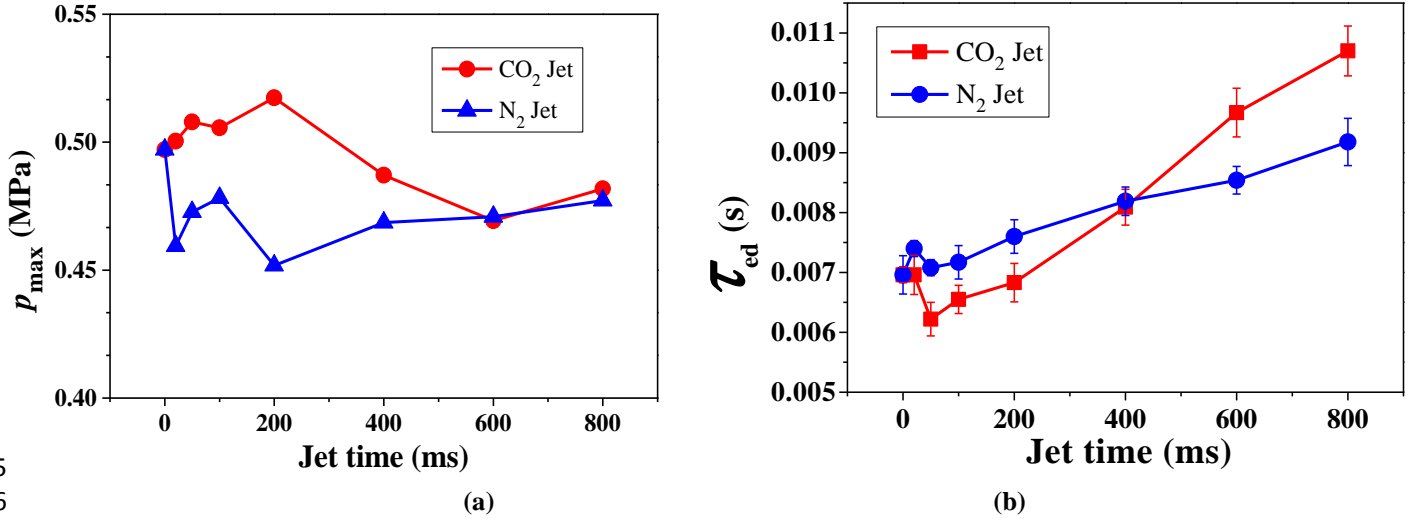
287

288 Similarly, Fig. 8 presents the results with N_2 turbulence. With increasing t_{J0} from 0 to 800 ms,
 289 p_{\max} is generally decreased for cases of $p_{J0}/p_0 = 5$ and 12.5. Only a slightly increase of p_{\max} is ob-
 290 served for $p_{J0}/p_0 = 8.3$. Figure 8b also indicates that, although τ_e experiences fluctuation with the

291 increase of t_{J0} (0 to 50 ms), an increasing behavior of τ_e is generally observed. These results thus
 292 show that the suppression effect of N_2 jet on p_{max} and τ_e is more apparent than that by using CO_2 .

293

294 3.4 Comparison between CO_2 and N_2 injections



295

296

297

Fig. 9 p_{max} and τ_e as a function of t_{J0} for the case of $p_0 = 40$ kPa and $p_{J0} = 500$ kPa.

298

299 Figure 9 compares the explosion parameters with t_{J0} variation between the CO_2 and N_2 jet tur-
 300 bulence. The initial condition is kept the same (i.e., $p_0 = 40$ kPa and $p_{J0} = 500$ kPa). The results in-
 301 dicate that p_{max} is lower while τ_e is longer under the effect of N_2 turbulence when t_{J0} is less than 400
 302 ms. As t_{J0} increases above 400 ms, τ_e is shorter and p_{max} is approaching that of the CO_2 .

303 Previous investigation [56] suggested that, at quiescent state with no turbulence, the effect of
 304 CO_2 dilution is more profound than N_2 dilution in reducing the values of combustion/explosion pa-
 305 rameters (including burning velocity, p_{max} , etc). However, the results obtained in this study is the
 306 opposite for $t_{J0} < 400$ ms, which illustrates the promoting effect by turbulence on the explosion is
 307 more profound than the suppression effect by gas dilution at shorter t_{J0} condition.

308

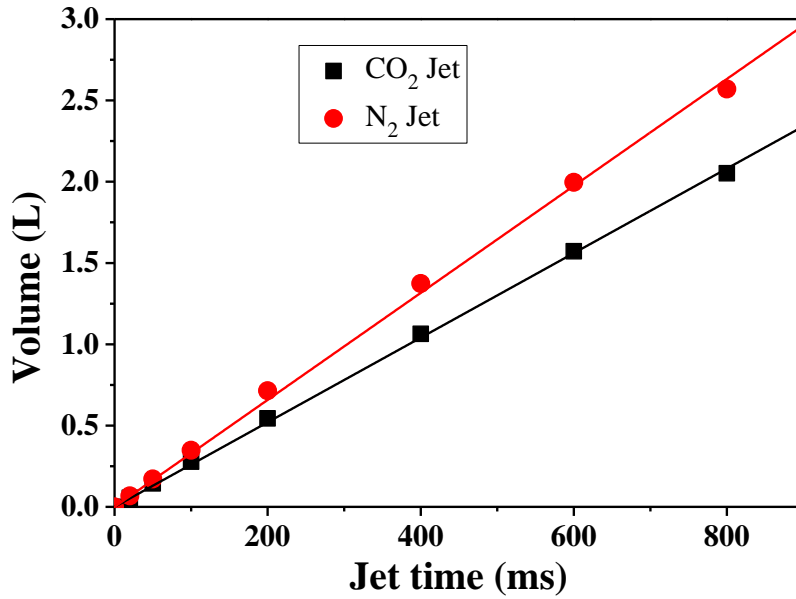


Fig.10 CO₂ and N₂ dilution as a function of t_{j0} for the case of $p_0 = 40$ kPa and $p_{j0} = 500$ kPa.

309

310

311

312

313

314

315

316

317

318

319

320

321

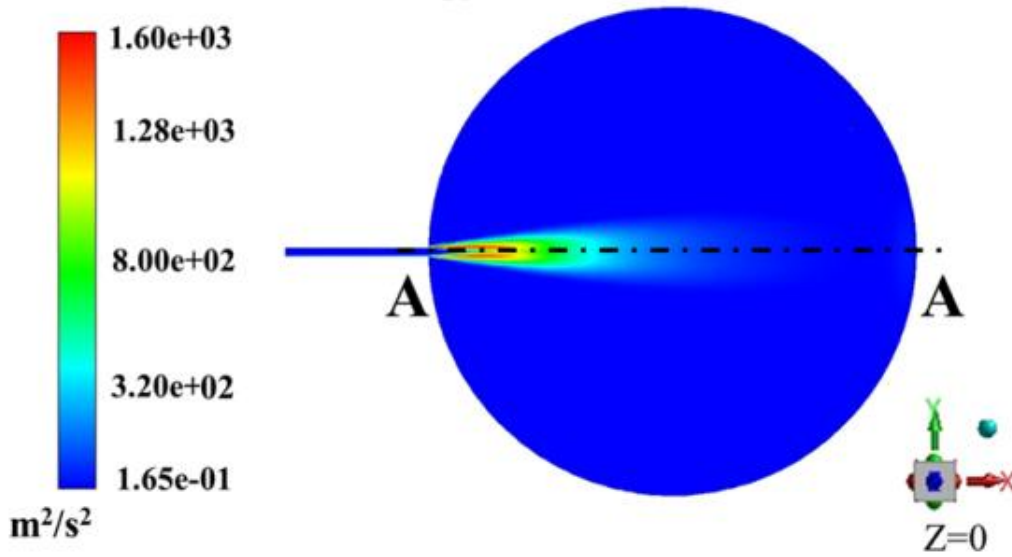
322

323

324

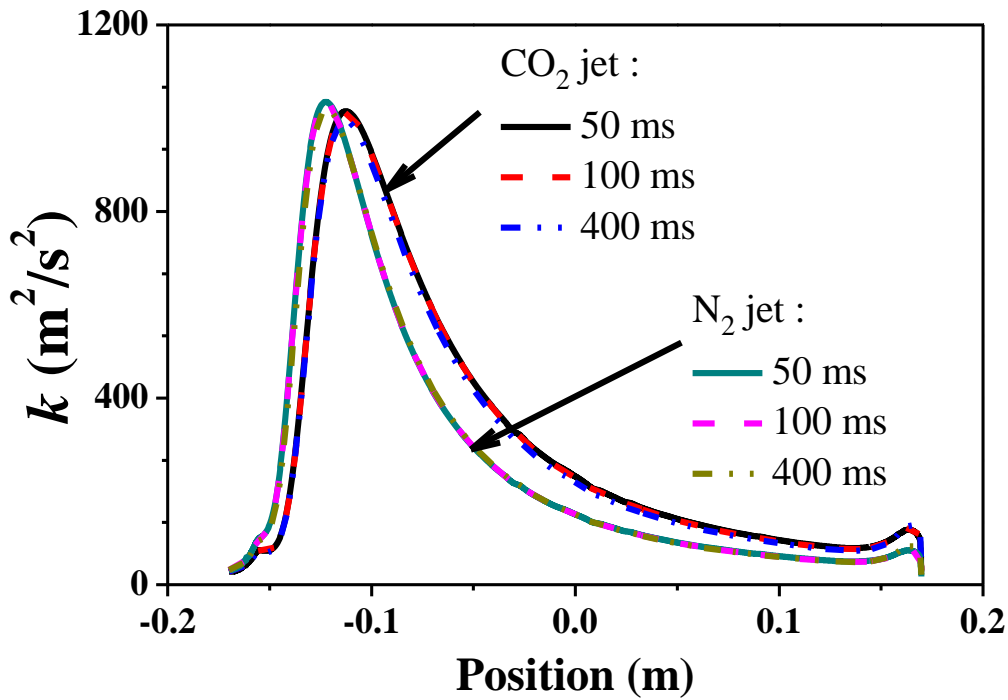
To clarify turbulence effects of CO₂ and N₂ jets on the explosion, numerical simulation using CFD package ANSYS Fluent 3D is performed. Reynolds averaged Navier-Stokes equations with the standard $k-\varepsilon$ turbulence model are used and solved using the SIMPLE algorithm. The domain is equivalent to the experiment, i.e., $V = 20$ L. The total number of elements is 1,055,928; increasing above this number of elements has no noticeable influence on the results. Figure 10 exhibits the volumes of CO₂ and N₂ injection at different t_{j0} from 0 to 800 ms for the case of $p_{j0}/p_0 = 12.5$ in experiment. The relationship between CO₂ or N₂ dilution and t_{j0} can be described as $V_{\text{CO}_2}(\text{L}) = 0.0026t_{j0}(\text{ms})$ and $V_{\text{N}_2}(\text{L}) = 0.0033t_{j0}(\text{ms})$, and the values of linearly dependent coefficient R^2 are calculated as 0.999 and 0.998, accordingly. An approximately linear relation between the inject flow and t_{j0} is assumed and hence, the jet entrance applies velocity-inlet boundary. To ensure the amount of gas injection in simulation is consistent with that in experiment, the jet entrance velocity is set as 162 m/s and 172 m/s for CO₂ and N₂ jet, respectively. The difference is due to the molecular weight of those gases under the same p_{j0}/p_0 .

Turbulent Kinetic Energy (k)



325
326
327

(a)



328
329
330
331
332
333

(b)

Fig. 11 Turbulent kinetic energy for CO_2 and N_2 jet with $p_0 = 40$ kPa and $p_{j0} = 500$ kPa. a) The turbulent kinetic energy field of CO_2 jet for $t_{j0} = 50$ ms; b) Turbulent kinetic energy along centerline for different t_{j0} .

334 Figure 11a shows the turbulent kinetic energy (k) contour using CO_2 jet with $t_{j0} = 50$ ms. The
335 axial distributions along the horizontal centerline (A-A) are shown in Fig. 11b for different t_{j0} . “0”

336 refers to the center of the 20-L spherical chamber. From the simulations, the turbulent kinetic ener-
337 gy plots for each corresponding CO₂ or N₂ jets coincide almost with each other regardless of t_{j0} .
338 Besides, it is indeed found that the k only depends on p_{j0}/p_0 . The turbulent kinetic energy is about
339 35 % greater for CO₂ jet than that of N₂ for the most places in the chamber particularly near the jet
340 entrance. Therefore, for $t_{j0} < 400$ ms, the CO₂ turbulence effect is more prominent than that of N₂
341 turbulence, enhancing explosion over the dilution effect. In contrast, the unreactive gas dilution in-
342 creases notably when $t_{j0} > 400$ ms and the prohibiting effect becomes more significant than the
343 turbulence promoting effect on the explosion behavior. This result helps to explain trends in Fig. 9.

344 This work presents experimental and numerical results of the turbulence effect on the explo-
345 sion behavior in methane-oxygen mixtures, the competing mechanism between turbu-
346 lence-enhanced effect and explosion-prohibited effect by added gases is clarified, those results may
347 contribute towards forming a more in-depth understanding of the real explosion process considering
348 turbulent condition.

349

350 4 Conclusion

351 In this study, two explosion characteristics, namely the maximum explosion pressure p_{\max} and
352 the explosion time τ_e , are measured experimentally using a standard 20-L spherical explosion vessel
353 for methane-oxygen mixtures at quiescent state and under the influence of initial turbulence. The
354 latter is generated by the injection of different gases (O₂, CO₂ and N₂) into the spherical chamber.
355 Turbulence intensity is controlled by changing the ratio of initial gas jet and chamber pressures
356 p_{j0}/p_0 . The following summarizes the findings:

357 (1) At quiescent state, adding the amount of O₂ into CH₄-2O₂ mixture increases the maximum
358 of overpressure but it reduces the pressure rise rate.

359 (2) There is a competition between explosion enhancing effect by turbulence and explosion
360 prohibiting effect by the injected gas dilution, both influencing the explosion behavior of me-
361 thane-oxygen mixtures in the confined chamber.

362 (3) By introducing O₂ jet turbulence, p_{\max} increases with increasing t_{J0} . τ_e is greatly reduced for
363 t_{J0} varying from 0 to 200 ms for $p_{J0}/p_0 = 12.5$ and 0 to 400 ms for $p_{J0}/p_0 = 8.3$. Longer t_{J0} renders the
364 chemical reaction rate slow.

365 (4) The turbulence intensity of CO₂ is more profound than that of N₂ jet. Hence, both p_{\max} and
366 τ_e are promoted by CO₂ turbulence for cases when t_{J0} is relatively short. At longer t_{J0} (e.g., $t_{J0} > 400$
367 ms), the effect of CO₂ dilution dominating the explosion behavior becomes more apparent than N₂
368 dilution.

369 Future research will focus on the interaction between turbulence and leading shock of the ex-
370 plosion and its effect on the explosion process by applying high-speed Schlieren camera, laser di-
371 agnostic apparatus (e.g., PIV) is to be employed to explore the detailed turbulent flow field on the
372 explosion process.

373

374 **Acknowledgment**

375 This work is supported by the National Natural Science Foundation of China – China (Grant Nos.:
376 91741114 and 11772199).

377

378

379

References:

380 [1] MacDonald G J. The future of methane as an energy resource. Annual Review of Energy 1990;

381 15: 53-83.

382 [2] Zhu D L, Egolfopoulos F N, Law C K. Experimental and numerical determination of laminar

- 383 flame speeds of methane/(Ar, N₂, CO₂)-air mixtures as function of stoichiometry, pressure, and
384 flame temperature. Symposium (International) on Combustion 1989; 22(1): 1537-45.
- 385 [3] Chen Z. Effects of hydrogen addition on the propagation of spherical methane/air flames: A
386 computational study. Int J Hydrogen Energ 2009; 34(15): 6558-67.
- 387 [4] Gabet K N, Shen H, Patton R A, Fuest F, Sutton J A. A comparison of turbulent dimethyl
388 ether and methane non-premixed flame structure. Proc Combust Inst 2013; 34(1): 1447-54.
- 389 [5] Chen Z, Qin X, Ju Y, Zhao Z, Chaos M, Dryer F L. High temperature ignition and combustion
390 enhancement by dimethyl ether addition to methane – air mixtures. Proc Combust Inst 2007;
391 31(1): 1215-22.
- 392 [6] Mitu M, Giurcan V, Razus D, Oancea D. Inert gas influence on the laminar burning velocity
393 of methane-air mixtures. J Hazard Mater 2017; 321: 440-8.
- 394 [7] Mitu M, Giurcan V, Razus D, Oancea D. Inert Gas Influence on Propagation Velocity of Me-
395 thane-air Laminar Flames. Revista de Chimie (Bucharest) 2018; 69(1): 196-200.
- 396 [8] Mitu M, Giurcan V, Razus D, Prodan M, Oancea D. Propagation indices of methane-air ex-
397 plosions in closed vessels. J Loss Prevent Proc 2017; 47: 110-9.
- 398 [9] Mitu M, Prodan M, Giurcan V, Razus D, Oancea D. Influence of inert gas addition on propa-
399 gation indices of methane – air deflagrations. Process Saf Environ 2016; 102: 513-22.
- 400 [10] Razus D, Mitu M, Giurcan V, Oancea D. Propagation indices of methane-nitrous oxide flames
401 in the presence of inert additives. J Loss Prevent Proc 2017; 49: 418-26.
- 402 [11] Hu E, Jiang X, Huang Z, Iida N. Numerical study on the effects of diluents on laminar burning
403 velocity of methane-air flames. Energ Fuel 2012; 26: 4242-52.
- 404 [12] Hu E, Li X, Meng X, Chen Y, Cheng Y, Xie Y, Huang Z. Laminar flame speeds and ignition
405 delay times of methane – air mixtures at elevated temperatures and pressures. Fuel 2015; 158:

- 406 1-10.
- 407 [13] Zhang B, Chang X Y, Bai C H. End-wall ignition of methane-air mixtures under the effects of
408 CO₂/Ar/N₂ fluidic jets. *Fuel* 2020; 270: 117485.
- 409 [14] Mitu M, Giurcan V, Razus D, Oancea D. Influence of Initial Pressure and Vessel' s Geometry
410 on Deflagration of Stoichiometric Methane - Air Mixture in Small-Scale Closed Vessels. *En-
411 ergy Fuels* 2020; 34(3): 3828-35.
- 412 [15] Zhang B, Liu H, Yan B, Ng H D. Experimental study of detonation limits in methane-oxygen
413 mixtures: Determining tube scale and initial pressure effects. *Fuel* 2020; 259: 116220.
- 414 [16] Zhang B, Liu H, Li Y C. The effect of instability of detonation on the propagation modes near
415 the limits in typical combustible mixtures. *Fuel* 2019; 253: 305-10.
- 416 [17] Zhang B, Liu H. Theoretical prediction model and experimental investigation of detonation
417 limits in combustible gaseous mixtures. *Fuel* 2019; 258: 116132.
- 418 [18] Zhang B, Liu H. The effects of large scale perturbation-generating obstacles on the propaga-
419 tion of detonation filled with methane-oxygen mixture. *Combust Flame* 2017; 182: 279-87.
- 420 [19] Zhang B. The influence of wall roughness on detonation limits in hydrogen-oxygen mixture.
421 *Combust Flame* 2016; 169: 333-9.
- 422 [20] Starr A, Lee J H S, Ng H D. Detonation limits in rough walled tubes. *Proc Combust Inst* 2015;
423 35(2): 1989-96.
- 424 [21] Lee J H S, Jesuthasan A, Ng H D. Near limit behavior of the detonation velocity. *Proc Com-
425 bust Inst* 2013; 34: 1957-63.
- 426 [22] Gao Y, Lee J H S, Ng H D. Velocity fluctuations near the detonation limits. *Combust Flame*
427 2014; 161(11): 2982-90.
- 428 [23] Zhang B, Liu H, Yan B J. Effect of acoustically absorbing wall tubes on the near-limit detona-

- 429 tion propagation behaviors in a methane-oxygen mixture. *Fuel* 2019; 236: 975-83.
- 430 [24] Zhang B, Liu H, Yan B J. Investigation on the detonation propagation limit criterion for me-
431 thane-oxygen mixtures in tubes with different scales. *Fuel* 2019; 239: 617-22.
- 432 [25] Grabarczyk M, Teodorczyk A, Di Sarli V, Di Benedetto A. Effect of initial temperature on the
433 explosion pressure of various liquid fuels and their blends. *J Loss Prevent Proc* 2016; 44: 775-9.
- 434 [26] Sanchirico R, Di Sarli V, Russo P, Di Benedetto A. Effect of the nozzle type on the integrity
435 of dust particles in standard explosion tests. *Powder Technol* 2015; 279: 203-8.
- 436 [27] Sanchirico R, Russo P, Saliva A, Doussot A, Di Sarli V, Di Benedetto A. Explosion of
437 lycopodium-nicotinic acid-methane complex hybrid mixtures. *J Loss Prevent Proc* 2015; 36:
438 507-10.
- 439 [28] Zhang B, Ng H D. An experimental investigation of the explosion characteristics of dimethyl
440 ether-air mixtures. *Energy* 2016; 107: 1-8.
- 441 [29] Shen X B, Zhang B, Zhang X L, Wu S Z. Explosion behaviors of mixtures of methane and air
442 with saturated water vapor. *Fuel* 2016; 177: 15-8.
- 443 [30] Zhang B, Ng H D. Explosion behavior of methane-dimethyl ether/air mixtures. *Fuel* 2015; 157:
444 56-63.
- 445 [31] Zhang B, Shen X B, Pang L. Effects of argon/nitrogen dilution on explosion and combustion
446 characteristics of dimethyl ether-air mixtures. *Fuel* 2015; 159: 646-52.
- 447 [32] Di Benedetto A, Cammarota F, Di Sarli V, Salzano E, Russo G. Reconsidering the flammabil-
448 ity diagram for CH₄/O₂/N₂ and CH₄/O₂/CO₂ mixtures in light of combustion-induced Rapid
449 Phase Transition. *Chem Eng Sci* 2012; 84(0): 142-7.
- 450 [33] Di Benedetto A, Cammarota F, Di Sarli V, Salzano E, Russo G. Anomalous behavior during
451 explosions of CH₄ in oxygen-enriched air. *Combust Flame* 2011; 158(11): 2214-9.

- 452 [34] Dorofeev S B. Flame acceleration and explosion safety applications. Proc Combust Inst 2011;
453 33(2): 2161-75.
- 454 [35] Di Benedetto A, Di Sarli V, Salzano E, Cammarota F, Russo G. Explosion behavior of
455 CH₄/O₂/N₂/CO₂ and H₂/O₂/N₂/CO₂ mixtures. Int J Hydrogen Energ 2009; 34(16): 6970-8.
- 456 [36] Mogi T, Horiguchi S. Explosion and detonation characteristics of dimethyl ether. J Hazard
457 Mater 2009; 164(1): 114-9.
- 458 [37] Wang D, Ji C, Wang S, Yang J, Tang C. Experimental investigation on near wall ignited lean
459 methane/hydrogen/air flame. Energy 2019; 168: 1094-103.
- 460 [38] Ma Q, Zhang Q, Chen J, Huang Y, Shi Y. Effects of hydrogen on combustion characteristics
461 of methane in air. Int J Hydrogen Energ 2014; 39(21): 11291-8.
- 462 [39] Wierzba I, Kilchyk V. Flammability limits of hydrogen-carbon monoxide mixtures at moder-
463 ately elevated temperatures. Int J Hydrogen Energ 2001; 26(6): 639-43.
- 464 [40] Di Sarli V, Di Benedetto A, Long E J, Hargrave G K. Time-Resolved Particle Image
465 Velocimetry of dynamic interactions between hydrogen-enriched methane/air premixed flames
466 and toroidal vortex structures. Int J Hydrogen Energ 2012; 37(21): 16201-13.
- 467 [41] Di Sarli V, Di Benedetto A. Effects of non-equidiffusion on unsteady propagation of hydro-
468 gen-enriched methane/air premixed flames. Int J Hydrogen Energ 2013; 38(18): 7510-8.
- 469 [42] Mitu M, Brandes E, Hirsch W. Ignition temperatures of combustible liquids with increased
470 oxygen content in the (O₂ + N₂) mixture. J Loss Prevent Proc 2019; 62: 103971.
- 471 [43] Shen X, Zhang N, Shi X, Cheng X. Experimental studies on pressure dynamics of C₂H₄/N₂O
472 mixtures explosion with dilution. Appl Therm Eng 2019; 147: 74-80.
- 473 [44] Zhou Q, Cheung C S, Leung C W, Li X, Huang Z. Effects of diluents on laminar burning
474 characteristics of bio-syngas at elevated pressure. Fuel 2019; 248: 8-15.

- 475 [45] Mitu M, Brandes E, Hirsch W. Mitigation effects on the explosion safety characteristic data of
476 ethanol/air mixtures in closed vessel. *Process Saf Environ* 2018; 117: 190-9.
- 477 [46] Di Benedetto A, Cammarota F, Di Sarli V, Salzano E, Russo G. Effect of diluents on rapid
478 phase transition of water induced by combustion. *Aiche J* 2012; 58(9): 2810-9.
- 479 [47] Di Sarli V, Di Benedetto A, Russo G, Jarvis S, Long E J, Hargrave G K. Large Eddy Simula-
480 tion and PIV Measurements of Unsteady Premixed Flames Accelerated by Obstacles. *Flow*
481 *Turbul Combust* 2009; 83(2): 227-50.
- 482 [48] Di Sarli V, Di Benedetto A, Russo G. Sub-grid scale combustion models for large eddy simu-
483 lation of unsteady premixed flame propagation around obstacles. *J Hazard Mater* 2010;
484 180(1-3): 71-8.
- 485 [49] Di Benedetto A, Garcia-Agreda A, Russo P, Sanchirico R. Combined Effect of Ignition Ener-
486 gy and Initial Turbulence on the Explosion Behavior of Lean Gas/Dust-Air Mixtures. *Ind Eng*
487 *Chem Res* 2012; 51(22): 7663-70.
- 488 [50] Sun Z, Li G. Turbulence influence on explosion characteristics of stoichiometric and rich hy-
489 drogen/air mixtures in a spherical closed vessel. *Energ Convers Manage* 2017; 149: 526-35.
- 490 [51] Bauwens C R, Dorofeev S B. Effect of initial turbulence on vented explosion overpressures
491 from lean hydrogen-air deflagrations. *Int J Hydrogen Energ* 2014; 39(35): 20509-15.
- 492 [52] Kundu S K, Zanganeh J, Eschebach D, Badat Y, Moghtaderi B. Confined explosion of me-
493 thane-air mixtures under turbulence. *Fuel* 2018; 220: 471-80.
- 494 [53] Zhang Y, Cao W, Shu C, Zhao M, Yu C, Xie Z, Liang J, Song Z, Cao X. Dynamic hazard
495 evaluation of explosion severity for premixed hydrogen-air mixtures in a spherical pressure
496 vessel. *Fuel* 2020; 261:116433.
- 497 [54] Peng H, Huang Y, Deiterding R, Luan Z, Xing F, You Y. Effects of jet in crossflow on flame

498 acceleration and deflagration to detonation transition in methane-oxygen mixture. *Combust*
499 *Flame* 2018; 198: 69-80.

500 [55] Wang Z R, Ni L, Liu X, Jiang J C, Wang R. Effects of N₂/CO₂ on explosion characteristics of
501 methane and air mixture. *J Loss Prevent Proc* 2014; 31: 10-5.

502 [56] Paidi S K, Bhavaraju A, Akram M, Kumar S. Effect of N₂/CO₂ dilution on laminar burning
503 velocity of H₂-air mixtures at high temperatures. *Int J Hydrogen Energ* 2013; 38(31):
504 13812-21.

505 [57] Chen Z, Qin M, Xu B, Ju Y G, Liu F S. Studies of radiation absorption on flame speed and
506 flammability limit of CO₂ diluted methane flames at elevated pressures. *Proc Combust Inst*
507 2007; 31(2): 2693-700.

508

The effects of pre-ignition turbulence by gas jets on the explosion behavior of methane-oxygen mixtures

Xinyu Chang¹, Bo Zhang^{2†}, Hoi Dick Ng³, Chunhua Bai¹

¹Beijing Institute of Technology
State Key Laboratory of Explosion Science and Technology, Beijing 100081, China

²Shanghai Jiao Tong University
School of Aeronautics and Astronautics, Shanghai, 200240, China

³Concordia University
Department of Mechanical, Industrial and Aerospace Engineering
Montréal, QC, H3G 1M8, Canada

Declaration of interests

The authors declare that they have no known competing financial interests or personal relationships that could have appeared to influence the work reported in this paper.

The authors declare the following financial interests/personal relationships which may be considered as potential competing interests:

CRedit authorship contribution statement

Xinyu Chang: Investigation

Bo Zhang: Investigation, Validation, Writing - review & editing, Methodology

Hoi Dick Ng: Validation , Writing - review & editing

Chunhua Bai: Investigation, Resources, Funding acquisition, Supervision,